Journal of Interdisciplinary Mathematics
ISSN: 0972-0502 (Print), ISSN: 2169-012X (Online)
Vol. 29 (2026), No. 9, pp. 2853–2863
DOI : 10.47974/JIM-2711

Nonlinear fractional diffusion model for image denoising and deblurring

Santosh Kumar †
Department of Mathematics & Data Science
Sharda School of Engineering & Science
Sharda University
Greater Noida 201310
Uttar Pradesh
India

Khursheed Alam *
Department of Mathematics & Data Science
The A. H. Siddiqi Centre for Advanced Research in Applied Mathematics & Physics (CARAMP)
Sharda University
Greater Noida 201310
Uttar Pradesh
India

Abstract

The most difficult and fundamental obstacles in image processing are reducing blur and noise in blurred noisy images. In this paper, we present a nonlinear fractional diffusion model for removing blur and noise in blurred noisy images. The fractional model is highly effective at eliminating noise while preserving edges, making it ideal for managing heavily noisy images corresponding to classical derivatives. The diffusion models are discretized by an explicit scheme. The improved signal-to-noise ratio (ISNR), which measures the smoothness of the restored images for numerical outcomes, is used.

Subject Classification (2020): *65M06, 76R50, 68U10.*

Keywords: *Partial differential equation, Diffusion model, Fractional diffusion model, Discrete scheme, ISNR values, Image processing.*

† *E-mail:* **skykumar87@gmail.com**
* *E-mail:* **khursheed.alam@sharda.ac.in (Corresponding Author)**

© Taru Publications

1. Introduction

Recently, many researchers have worked on image denoising and deblurring in the last few decades. Still, image denoising remains a challenging problem for researchers. The major challenge is to recover the texture of the image while preserving all the edges. The blurred and noise-corrupted image u_0 : Ω→R is defined as

$$u_0 = k * u + r.$$

Here, Ω is a bounded open domain of R^2, original image u, additive Gaussian white noise r which contains mean zero, variance σ^2 and a Gaussian blurred kernel denoted by k.

The PDE-based anisotropic diffusion models for edge preservation, as well as for the reduction of the blocky effect. The first approach in this regard is to remove noise by the diffusion proposed by Perona and Malik [1]. Catte et al. [2] proposed an improved PM model for images. This model is based on the scale-space theory given by Witkin [3]. The diffusion tensor-based model for image restoration was proposed by Weickert [4]. Kumar, Sarfaraz, and Ahmad [5] proposed a wavelet-based approach for eliminating additive noise. They employed a discrete wavelet transform to break down the noisy data before using a wavelet filter to recreate it. Various techniques for image restoration were proposed by the researchers in [6, 7, 8, 9].

Fractional calculus is as old as Newton-Leibnitz calculus. However, its applications to real-world systems were in doubt for a long time [10]. The concept of conformable fractional derivative (CFD) was first given by Khalil et al. [11]. The fractional diffusion model for removing noise is proposed by Kumar, Alam, and Chauhan [12]. Many researchers are interested in using the fractional derivative for image denoising, and many applications of fractional derivatives and other approaches are given in [13, 14, 15]. In this paper, the PDE-based anisotropic fractional diffusion model is proposed for edge detection and image restoration. The improved model contains the time-fractional derivative with a diffusivity parameter. The results are given in Table 1 and Figures 1-6.

2. Conformable Fractional Derivative

Khalil et al. [11] introduced a computational relationship with the CFD that satisfies properties such as the chain, product, and quotient rules for the first derivative. The conformable derivative is very effective and applicable in many fields such as stochastic processes [16], quantum mechanics [17], time scale problems [18], and Newton mechanics [19], etc. Zhao and Luo [20] proposed the physical interpretation, and many applications see reference [21, 22].

The CFD is defined by the function u: $(0,\infty) \rightarrow$ R such that

$$U_\alpha(u)(t) = U_\alpha u(t) = \lim_{\varepsilon\to 0} \frac{u\left(t+\varepsilon t^{1-\alpha}\right)-u(t)}{\varepsilon},$$

provided the limit exists for all values t >0 and $\alpha \in (0,1)$.

The function u is represented α-differentiable in $(0, a)$ for some $a > 0$ and can also be written in another form:

$U_\alpha u(0) = \lim_{t\to 0^+} U_\alpha u(t)$ and it is similar to $U_\alpha u(0) = t^{1-\alpha}u'(t)$, where $u'(t)$ is the classical derivative with respect to t.

3. Denoising-Based Time-Fractional Diffusion Algorithm

An energy-dissipating procedure to find the minimum of an energy function is linked to anisotropic diffusion. Let t represent the time and ζ represent the diffusion coefficient; the PM model [1] is as follows:

$$u_t = \nabla \cdot (\zeta(|\nabla u|)\nabla u),$$

where $u_t = \frac{\partial u}{\partial t}$ and the gradient operator represented by ∇. Anisotropic diffusion has advantages such as edge preservation and intra-regional smoothing. However, it frequently results in the staircase effect [23].

The 2-dimensional additive noise and blurred diffusion model was studied by Welk et al. [24]. They introduced the energy-minimizing functional, such as:

$$f(u) = \int_\Omega \varphi(|\nabla u|^2)\, dx + \frac{\lambda}{2}\int_\Omega (k * u - u_0)^2\, dx \tag{3.1}$$

The Euler-Lagrange equation is:

$$0 = -\nabla \cdot (\varphi(|\nabla u|^2)\nabla u) + \lambda\, k * (k * u - u_0), x\epsilon\Omega. \tag{3.2}$$

$$\frac{\partial u}{\partial n} = 0\ x \in \partial\Omega,$$

where n is the outward normal to $\partial\Omega$, and $\partial\Omega$ is the border of Ω.

By the gradient descent method, the above equation leads to a diffusion model:

$$\mathrm{u_t} = \nabla \cdot (\zeta(|\nabla \mathrm{u}|^2)\nabla \mathrm{u}) - \lambda\, \mathrm{k} * (\mathrm{k} * \mathrm{u} - \mathrm{u_0}). \tag{3.3}$$

Here u_0 taken as an initial guess when $t = 0$ and the diffusivity $\zeta(s^2) = \varphi'(s^2)$.

The diffusivity ζ, the diffusion threshold parameter K, s is the gradient of the image, and $\zeta(\mathrm{s}^2)$ is a nonnegative function. The threshold parameter K is used to control the image enhancement. The Charbonnier diffusivity $\zeta(\mathrm{s}^2) = \frac{1}{\sqrt{1+(|\mathrm{s}|^2/\mathrm{K}^2)}}$, which is associated with $\varphi(\mathrm{s}^2) = \sqrt{\mathrm{K}^4 + \mathrm{K}^2\mathrm{s}^2} - \mathrm{K}^2$, [4, 25] is used in our numerical experiments.

The conformable fractional derivative is applicable to complex problems such as image restoration and edge detection [26, 27]. The model (3.3) converts into a fractional diffusion model such as:

$$u_t^\alpha = \nabla \cdot (\zeta(|\nabla u|^2)\nabla u) - \lambda\, k * (k * u - u_0). \tag{3.4}$$

Now, using the definition of the CFD given in Section 2, α is the fractional order derivative.

4. Discrete Scheme

In this section, we present a clear approach to discretizing both the anisotropic diffusion and the fractional anisotropic diffusion models. Let $u_{i,j}^n$

denote the approximation for the value $u(x_i, y_j, t_n)$. The spatial step sizes Δx and Δy are equal, and the time step size Δt is defined as well. We define the discrete approximations as $x_i = i\Delta x$ and $y_j = j\Delta y$ for $i, j = 1,2,3\ldots\ldots N$, where $N\Delta x = 1$, and $t_n = n\Delta t, n \geq 1$.

The discrete explicit scheme of the model (3.3) is:

$$u_{ij}^t = \frac{1}{2\Delta x}\left[\left(\zeta_{i+1,j}^n + \zeta_{i,j}^n\right)\left(u_{i+1,j}^n - u_{i,j}^n\right) - \left(\zeta_{i,j}^n + \zeta_{i-1,j}^n\right)\left(u_{i,j}^n - u_{i-1,j}^n\right)\right]$$
$$+ \frac{1}{2\Delta x}\left[\left(\zeta_{i,j+1}^n + \zeta_{i,j}^n\right)\left(u_{i,j+1}^n - u_{i,j}^n\right) - \left(\zeta_{i,j}^n + \zeta_{i,j-1}^n\right)\left(u_{i,j}^n - u_{i,j-1}^n\right)\right] -$$
$$\lambda\, k * \left(k * u_{ij}^n - u_{ij}^0\right).$$

The discrete explicit scheme of the fractional diffusion model (3.4) is:

$$u_{ij}^t = t^{\alpha-1}\frac{1}{2\Delta x}\left[\left[\left(\zeta_{i+1,j}^n + \zeta_{i,j}^n\right)\left(u_{i+1,j}^n - u_{i,j}^n\right) - \left(\zeta_{i,j}^n + \zeta_{i-1,j}^n\right)\left(u_{i,j}^n - u_{i-1,j}^n\right)\right] +\right.$$
$$t^{\alpha-1}\frac{1}{2\Delta x}\left[\left(\zeta_{i,j+1}^n + \zeta_{i,j}^n\right)\left(u_{i,j+1}^n - u_{i,j}^n\right) - \left(\zeta_{i,j}^n + \zeta_{i,j-1}^n\right)\left(u_{i,j}^n - u_{i,j-1}^n\right)\right] -$$
$$t^{\alpha-1}\lambda\, k * \left(k * u_{ij}^n - u_{ij}^0\right),$$

where the diffusivity $\zeta(|\nabla u|^2)$ is discretized by,

$$\zeta_{ij}^n = \varphi'\left(\left(\frac{u_{i+1,j}^n - u_{i-1,j}^n}{\Delta x}\right)^2 + \left(\frac{u_{i,j+1}^n - u_{i,j-1}^n}{\Delta x}\right)^2\right).$$

5. Numerical Implementation and Results

The original real grayscale images contain pixel values between 0 and 255 as given in Figure 1. For our numerical experiment, we reduce the pixel values between 0 and 1. The image is corrupted by the function normal imnoise (u, Gaussian, m, σ^2) in Matlab, where m is the mean and σ^2 is the variance. The parameters K = 5, $\lambda = 0.85$, t = 0.002, and $\Delta t/\Delta x^2 = 0.4$ are used in numerical experiments, see reference [28, 29, 30, 31].

For the level of noise, we use the signal-to-noise ratio (SNR), the blurred signal-to-noise ratio (BSNR), and check the clarity of the restored image by ISNR as follows:

$$\text{SNR} = \frac{\|u - \bar{u}\|_{L^2}}{\sigma} dB$$

where L^2 stands for L^2-norm, σ for noise and $\bar{u}$ is the mean.

$$\text{BSNR} = 10log_{10}\left(\frac{\sum_{i,j}^n [k * u_{ij} - (\bar{u})]}{\sum_{i,j}^n [r_{i,j}]^2}\right) dB,$$

where $\bar{u} = \sum_{i,j}^n \frac{u_{i,j}}{n^2}$.

$$\text{ISNR} = 10log_{10}\left(\frac{\sum_{i,j}^n [u_{ij} - (u_0)_{ij}]^2}{\sum_{i,j}^n [u_{i,j} - (u_{new})_{i,j}]^2}\right) dB,$$

where the restored image is u_{new}.

Figure 1 (a-b) represents the original images of pixel values 512 × 512, and Figure 1 (c) represents the original images of pixel values 1024 × 1024. Figures 2 (a) and 3 (a) denote blurred and noisy images with additive Gaussian white

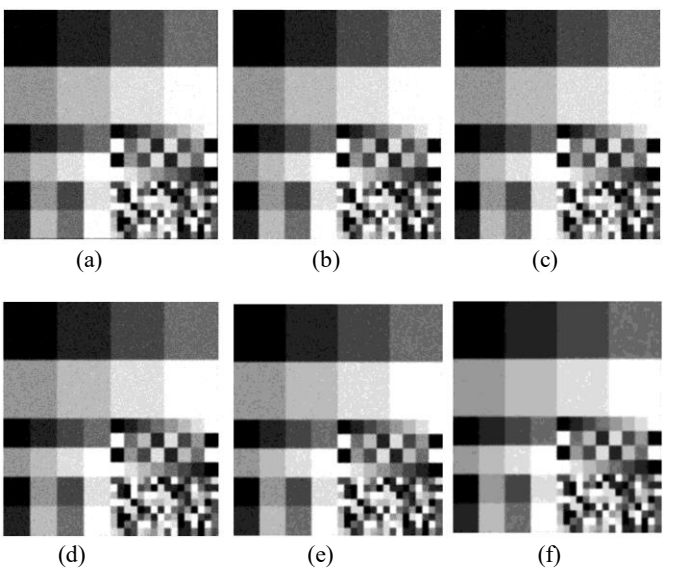
noise $\sigma^2 = 0.006, 0.008$, Gaussian blurred kernel of size 5 and blurring parameter 3, respectively, wherein their SNR=4.2772, 3.7041 and BSNR=12.3841, 11.1347. Figures 4 (a) and 5 (a) represent blurred and noisy images with additive Gaussian white noise $\sigma^2 = 0.006,0.008$, Gaussian blurred kernel of size 5 and blurring parameter 3, respectively, wherein their SNR=2.3631, 2.0465 and BSNR=6.9328, 5.6834. Figure 6 (a) represents blurred and noisy images with additive Gaussian white noise $\sigma^2 = 0.008$, a Gaussian blurred kernel of size 5, and a blurring parameter 3 with SNR=2.2717 and BSNR=6.8508.



(a) (b) (c)

Figure 1

(a)-(b) represent original grayscale images of pixel values 512 × 512; (c) represents the original image of pixel values 1024 × 1024.



(a) (b) (c)

(d) (e) (f)

Figure 2

(a) Blurred noisy image with ($\sigma^2 = 0.006$); (b) Restored image by model (3.3); (c-f) Restored by different fractional derivatives $\alpha = 0.7,0.5, 0.3$ and 0.1 by model (3.4), respectively.

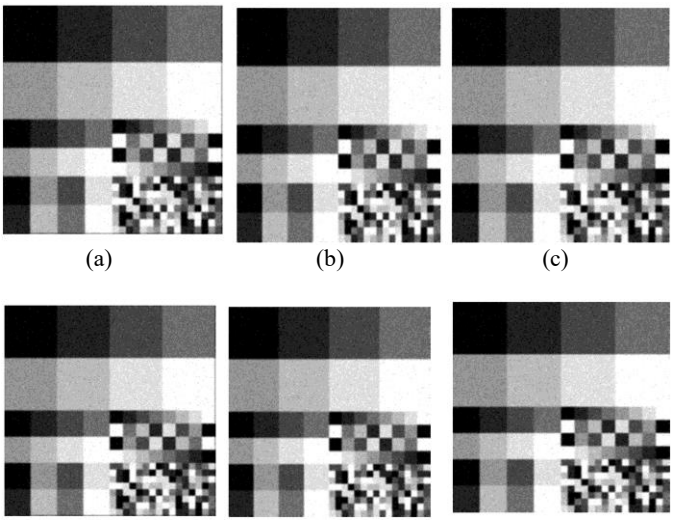


Figure 3

(a) Blurred noisy image with ($\sigma^2 = 0.008$); (b) Restored image by model (3.3); (c-f) Restored by different fractional derivatives $\alpha = 0.7, 0.5, 0.3$ and 0.1 by model (3.4), respectively.

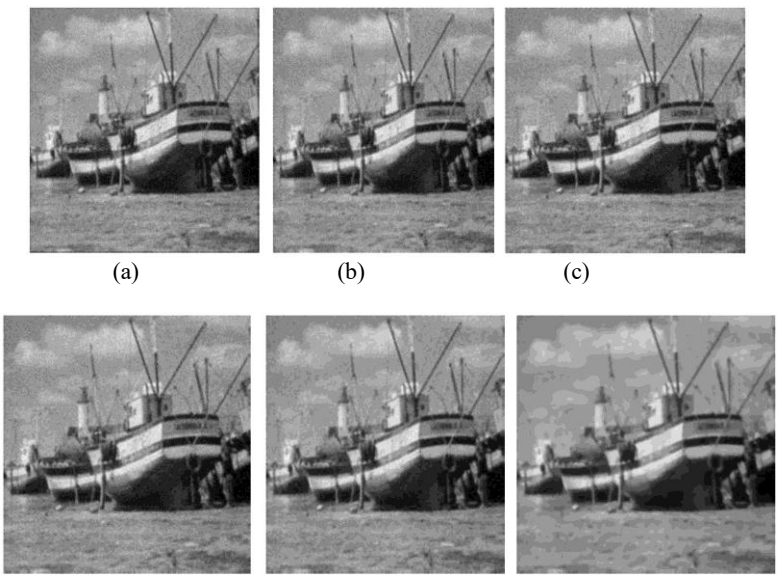


Figure 4

(a) Blurred noisy image with ($\sigma^2 = 0.006$); (b) Restored image by model (3.3); (c-f) Restored by different fractional derivatives $\alpha = 0.7, 0.5, 0.3$ and 0.1 by model (3.4), respectively.

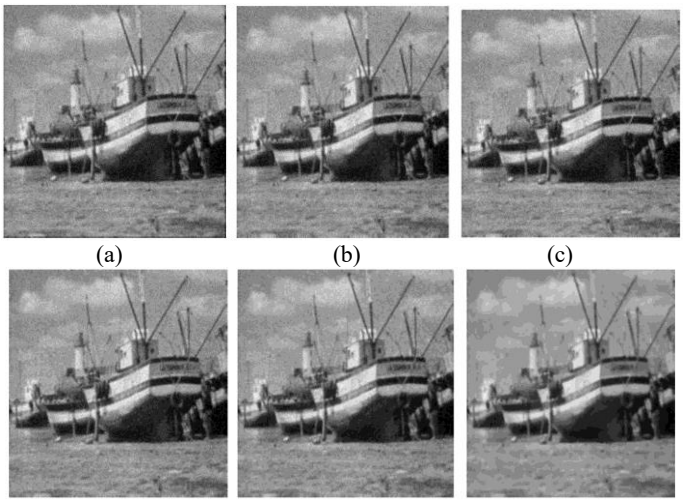


Figure 5
(a) Blurred noisy image with ($\sigma^2 = 0.008$); (b) Restored image by model (3.3); (c-f) Restored by different fractional derivatives α = 0.7,0.5, 0.3 and 0.1 by model (3.4) respectively.

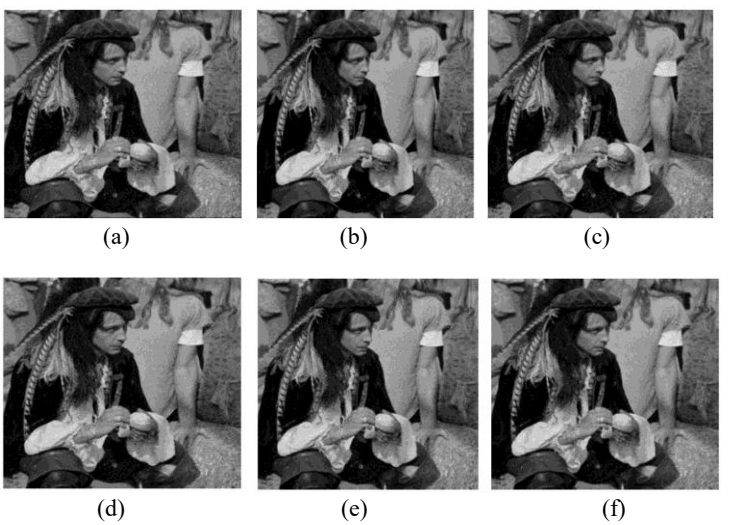


Figure 6
(a) Blurred noisy image with ($\sigma^2 = 0.008$); (b) Restored image by model (3.3); (c-f) Restored by different fractional derivatives α = 0.7,0.5, 0.3 and 0.1 by model (3.4), respectively.

Table 1

The results of fractional and classical diffusion models:

Restored images by (3.3)	ISNR values by (3.3)	Restored images by (3.4)	ISNR values by Model (3.4)			
			$\alpha = 0.7$	$\alpha = 0.5$	$\alpha = 0.3$	$\alpha = 0.1$
2(b)	0.7148	2(c-f)	0.9644	2.1848	3.6702	4.1858
3(b)	0.6722	3(c-f)	0.9168	2.2093	4.0042	4.8236
4(b)	0.7186	4(c-f)	0.9967	2.4546	4.1026	4.4210
5(b)	0.6824	5(c-f)	0.9446	2.4654	4.7986	5.2716
6(b)	0.2805	6(c-f)	0.2820	0.8147	2.3195	5.1529
No. of iterations	200	**No. of iterations**	50			

6. Conclusion

We shall see that the experimental results for different fractional orders significantly reduce the iteration step and yield a better ISNR value corresponding to the classical model. The fractional-order α is very efficient in numerical experiments. A very small fractional order α will provide more clarity, denoising, and deblurring of the image and better-preserved edges at a smaller number of iterations. To check the clarity of the restored image is checked by the ISNR value. A larger ISNR value of the images is a good result. The proposed model (3.4) has larger ISNR values corresponding to (3.3) at the small iteration numbers. It is observed that the proposed model contains good results in comparison to the other model (3.3). The fractional diffusion model provided fast process images during image restoration.

References

[1] P. Perona and J. Malik, "Scale space and edge detection using anisotropic diffusion," *IEEE Transactions on Pattern Analysis and Machine Intelligence*, vol. 12, no. 7, pp. 629–639 (1990).

[2] F. Catte, P.L. Lions, J.M. Morel and T. Coll, "Image selective smoothing and edge detection by nonlinear diffusion," *SIAM J. Numer. Anal*., vol. 29, no. 1, pp. 182-193 (1992).

[3] A. P. Witkin, "Scale-space filtering," *Proc. IJCAI Karlsruhe*, pp. 1019-1021 (1983).

[4] J. Weickert, "A Review of nonlinear diffusion filtering," *In scale space LNCS. Springer Berlin*, vol. 1252, pp. 3-28 (1997).

[5] S. Kumar, M. Sarfaraz, and M. K. Ahmad, "Denoising method based on wavelet coefficients via diffusion equation," *Iran. J. Sci. Technol.*

Trans. A: Sci., vol. 42, no. 2, pp. 721–726 (2018), doi: 10.1007/s40995-017-0228-7.

[6] L. Alvarez, P. L. Lions, and J. M. Morel, "Image selective smoothing and edge detection by nonlinear diffusion II," *SIAM J. Numer. Anal*., vol. 29, no. 3, pp. 845-866 (1992).

[7] S. Kumar, N. Kumar, and K. Alam, "A nonlinear anisotropic diffusion equation for image restoration with forward-backward diffusivities," *Recent Advances in Electrical & Electronic Engineering (Formerly Recent Patents on Electrical & Electronic Engineering)*, vol. 14, no. 4, pp. 428-434 (2021).

[8] A. Chauhan, S. Kumar, and Y. Karaca, "A new fractional-order derivative-based nonlinear anisotropic diffusion model for biomedical imaging," *Chaos Theory and Applications*, vol. 5, no. 3, pp. 198-206 (2023).

[9] A. D. Nagargoje, V. C. Borkar, and R. A. Muneshwar, "Analytical solutions and numerical simulation of COVID-19 fractional order mathematical model by Caputo and conformable fractional differential transform method," *J. Inf. Optim. Sci.,* vol. 44, no. 4, pp. 653–673 (2023), doi: 10.47974/JIOS-1219.

[10] R. Hermann, "Fractional Calculus, An Introduction for Physicists," *World Scientific Publishing Co. Pvt. Ltd*., 2nd Edition (2014).

[11] R. Khalil, M. Al Horani, A. Yousef, and M. Sabebah, "A new definition of Fractional Derivative," *Journal of Computational and Applied Mathematics*, vol. 264, pp. 65-70 (2014).

[12] S. Kumar, K. Alam, and A. Chauhan, "Fractional derivative based nonlinear diffusion model for image denoising," *SeMA, vol.* 79, pp. 355-364 (2022).

[13] T. Abdeljawad, "On conformable fractional calculus," *Journal of Computational and Applied Mathematics*, vol. 279, pp. 57-66 (2015).

[14] D. Avci, B. B. Iskender Eroğlu, and N. Özdemir, "Conformable heat equation on a radial symmetric plate," *Thermal Science,* vol. 21, no. 2, pp. 819–826 (2017), doi: 10.2298/TSCI160427302A.

[15] H. Günerhan, M. Yiğider, J. Manafian, and O. A. Ilhan, "Numerical solution of fractional order logistic equations via conformable fractional differential transform method," *J. Interdiscip. Math*., vol. 24, no. 5, pp. 1207–1220 (2021), doi: 10.1080/09720502.2021.1918319.

[16] Y. Cenesiz and A. Kurt, "The solutions of time and space conformable fractional heat equations with conformable Fourier transform," *Acta Univ. Sapientiae, Mathematica*, vol. 7, no. 2, pp. 130-140 (2015).

[17] D. R. Anderson and D. J. Ulness, "Properties of the Katugampola fractional derivative with potential application in quantum mechanics," *J. Math. Phys.,* vol. 56, no. 6, Art. no. 063502 (2015), doi: 10.1063/1.4922018.

[18] N. Benkhettou, S. Hassani, and D.F. Torres, "A conformable fractional calculus on arbitrary time scales," *Journal of King Saud University-Science*, vol. 28, no. 1, pp. 93-98 (2016).

[19] W. S. Chung, "Fractional Newton mechanics with conformable fractional derivative," *J. Comput. Appl. Math.*, vol. 290, pp. 150-158 (2015).

[20] D. Zhao and M. Luo, "General conformable fractional derivative and its physical interpretation," *Calcolo*, vol. 54, pp. 903-917 (2017).

[21] M. Bezziou and Z. Dehmani, "New integral operators for conformable fractional calculus with applications," *J. Interdiscip. Math.,* vol. 25, no. 4, pp. 927–940 (2022), doi: 10.1080/09720502.2021.1880138.

[22] A. A. Kilbas, H. M. Srivastava, and J. J. Trujillo, "Theory and Applications of Fractional Differential Equations," *North-Holland Mathematics Studies*, vol. 204, pp. 1-523 (2006).

[23] J. Bai and X. C. Feng, "Fractional order anisotropic diffusion for image denoising," *IEEE Trans. Image Process.,* vol. 16, pp. 2492-2502 (2007).

[24] M. Welk, D. Theis, T. Brox, and J. Weickert, "PDE-based deconvolution with forward-backward diffusivities and diffusion tensors," *In scale space, LNCS, Springer Berlin*, pp. 585-597 (2005).

[25] P. Charbonnier, L. Blanc-Féraud, G. Aubert, and M. Barlaud, "Two deterministic half-quadratic regularization algorithms for computed imaging," in *Proc. 1994 IEEE International Conference on Image Processing (ICIP)*, vol. 2, Austin, TX, USA, pp. 168–172 (Nov. 1994), doi: 10.1109/ICIP.1994.413553.

[26] R. W. Ibrahim, "A new image denoising model utilizing the conformable fractional calculus for multiplicative noise," *SN Appl. Sci.*, vol. 2, no. 32 (2020).

[27] H. W. Zhou, S. Yang, and S. Q. Zhang, "Conformable derivative approach to anomalous diffusion," *Physica A: Statistical Mechanics and its Applications,* vol. 491, pp. 1001-1013 (2018).

[28] M. Abu Hammad and R. Khalil, "Conformable fractional heat differential equation," *Int. J. Pure Appl. Math.,* vol. 94, no. 2, pp. 215–221 (2014), doi: 10.12732/ijpam.v94i2.8.

[29] T. F. Chan, G. H. Golub, and P. Mulet, "A nonlinear primal-dual method for total variation-based image restoration," *SIAM J. Sci. Comput*., vol. 20, no. 6, pp. 1964-1977 (1999).

[30] Q. Chang and Chern I-Liang, "Acceleration methods for total variation-based image denoising," *SIAM J. Sci. Comput*., vol. 25, no. 3, pp. 982-994 (2003).

[31] L. Lapidus and G.F. Pinder, "Numerical solution of partial differential equations in science and engineering," *SIAM Rev*., vol. 25, no. 4, pp. 581-582 (1983).

Received January, 2026